J|A|C|S
ARTICLES
Published on Web 07/21/2004

Molecular Clips Form Isostructural Dimeric Aggregates from Benzene to Water

Anxin Wu,[†,‡] Pritam Mukhopadhyay,[†] Arindam Chakraborty,[†] James C. Fettinger,[†] and Lyle Isaacs*[,†]

Contribution from the Department of Chemistry and Biochemistry, University of Maryland, College Park, Maryland 20742, and College of Chemistry, Central China Normal University, Wuhan, Hubei 430079, P.R. China

Received March 7, 2004; E-mail: LIsaacs@umd.edu

Abstract: We report the synthesis and characterization of eight C-shaped methylene-bridged glycoluril dimers (**1**−**8**) bearing hydrogen-bonding amide groups on their aromatic rings. Compounds **1**−**6** undergo tight dimerization in $CDCl_3$ solution ($K_s > 9 \times 10^5\ M^{-1}$); binary mixtures of **1**−**7** form mixtures of homodimers and heterodimers in moderately selective dimerization processes ($0.23 \leq K_{eq} \leq 768$; $0.253 \leq \chi_{AB} < 0.933$). The high affinity formation of **1·1**−**6·6** is due to the commensurate nature of the geometrical constraints imposed by the $\pi-\pi$ interactions and only two hydrogen bonds. The differential response of the strengths of the $\pi-\pi$ interactions and H-bonds of **2·2** to changes in solvent polarity—from C_6D_6 to D_2O—results in the formation of a solvent-independent isostructural aggregate that exhibits high affinity dimerization across the full range of solvents.

Introduction

Nature is replete with exquisite examples of macromolecular structures and their assemblies that possess well-defined catalytic and molecular recognition properties.[1] Examples include double-helical DNA, ribosomes, antibodies, cell membranes, and viruses. In folding and assembling these macromolecules, nature normally utilizes a combination of noncovalent interactions, including hydrogen bonds, metal−ligand interactions, electrostatic interactions, and the hydrophobic effect to achieve stability in either an aqueous or lipophilic environment. Inspired by nature, supramolecular chemists have learned to use hydrogen bonds, metal−ligand interactions, and the hydrophobic effect to prepare aggregates that are stable and structured under a specific set of conditions (e.g., solvent and temperature) and have begun to endow them with function.[2,3] Unlike biological systems that operate only under a well-defined set of conditions (e.g., 37 °C, pH 7.4, 150 mM salt), many applications of chemical systems would benefit greatly from the presence of a single well-defined supramolecular structure with high stability over a broad range of conditions. Such structurally invariant systems complement the behavior of dynamic assemblies that respond to changes in solvent composition.[4,5]

Several groups have prepared new hydrogen-bonding modules[6,7] that are robust, functionalizable, and tightly associated for use in advanced applications, including supramolecular polymers,[8,9] molecular capsules,[10] molecular constellations,[11] enantiomeric self-recognition,[9,12] unidirectional molecular rotors,[13] antibacterial nanotubes,[14] synthetic catalytic pores,[15] artificial β-sheets,[16] noncovalent regulators,[17] and molecular

[†] University of Maryland, College Park.
[‡] Central China Normal University.

(1) Stryer, L. *Biochemistry*; W. H. Freeman and Co.: New York, 1995.
(2) Meyer, E. A.; Castellano, R. K.; Diederich, F. *Angew. Chem., Int. Ed.* **2003**, *42*, 1210−1250. Balzani, V.; Credi, A.; Raymo, F. M.; Stoddart, J. F. *Angew. Chem., Int. Ed.* **2000**, *39*, 3348−3391. Prins, L. J.; Reinhoudt, D. N.; Timmerman, P. *Angew. Chem., Int. Ed.* **2001**, *40*, 2382−2426. Lehn, J.-M. *Supramolecular Chemistry*; VCH: Weinheim, 1995. Seidel, S. R.; Stang, P. J. *Acc. Chem. Res.* **2002**, *35*, 972−983.
(3) Rowan, S. J.; Cantrill, S. J.; Cousins, G. R. L.; Sanders, J. K. M.; Stoddart, J. F. *Angew. Chem., Int. Ed.* **2002**, *41*, 898−952.
(4) Lehn, J.-M. *Proc. Natl. Acad. Sci. U.S.A.* **2002**, *99*, 4763−4768.
(5) Prince, R. B.; Saven, J. G.; Wolynes, P. G.; Moore, J. S. *J. Am. Chem. Soc.* **1999**, *121*, 3114−3121. Mao, C.; Thalladi, V. R.; Wolfe, D. B.; Whitesides, S.; Whitesides, G. M. *J. Am. Chem. Soc.* **2002**, *124*, 14508−14509. Dolain, C.; Maurizot, V.; Huc, I. *Angew. Chem., Int. Ed.* **2003**, *42*, 2738−2740. Bharathi, P.; Zhao, H.; Thayumanavan, S. *Org. Lett.* **2001**, *3*, 1961−1964.
(6) Sijbesma, R. P.; Meijer, E. W. *Chem. Commun.* **2003**, 5−16. Beijer, F. H.; Sijbesma, R. P.; Kooijman, H.; Spek, A. L.; Meijer, E. W. *J. Am. Chem. Soc.* **1998**, *120*, 6761−6769. Corbin, P. S.; Zimmerman, S. C.; Thiessen, P. A.; Hawryluk, N. A.; Murray, T. J. *J. Am. Chem. Soc.* **2001**, *123*, 10475−10488. Corbin, P. S.; Zimmerman, S. C. *J. Am. Chem. Soc.* **2000**, *122*, 3779−3780. Corbin, P. S.; Zimmerman, S. C. *J. Am. Chem. Soc.* **1998**, *120*, 9710−9711. Zeng, H.; Yang, X.; Brown, A. L.; Martinovic, S.; Smith, R. D.; Gong, B. *Chem. Commun.* **2003**, 1556−1557. Gong, B. *Chem. Eur. J.* **2001**, *7*, 4337−4342. Zeng, H.; Miller, R. S.; Flowers, R. A., II; Gong, B. *J. Am. Chem. Soc.* **2000**, *122*, 2635−2644. Mogck, O.; Bohmer, V.; Vogt, W. *Tetrahedron* **1996**, *52*, 8489−8496. Vysotsky, M. O.; Thondorf, I.; Bohmer, V. *Chem. Commun.* **2001**, 1890−1891. Vysotsky, M. O.; Bolte, M.; Thondorf, I.; Bohmer, V. *Chem. Eur. J.* **2003**, *9*, 3375−3382. Archer, E. A.; Sochia, A. E.; Krische, M. J. *Chem. Eur. J.* **2001**, *7*, 2059−2065. Schmuck, C.; Wienand, W. *J. Am. Chem. Soc.* **2003**, *125*, 452−459. Zadmard, R.; Junkers, M.; Schrader, T.; Grawe, T.; Kraft, A. *J. Org. Chem.* **2003**, *68*, 6511−6521. Bisson, A. P.; Carver, F. J.; Eggleston, D. S.; Haltiwanger, R. C.; Hunter, C. A.; Livingstone, D. L.; McCabe, J. F.; Rotger, C.; Rowan, A. E. *J. Am. Chem. Soc.* **2000**, *122*, 8856−8868. Brammer, S.; Luning, U.; Kuhl, C. *Eur. J. Org. Chem.* **2002**, 4054−4062. Zhao, X.; Wang, X.-Z.; Jiang, X.-K.; Chen, Y.-Q.; Li, Z.-T.; Chen, G.-J. *J. Am. Chem. Soc.* **2003**, *125*, 15128−15139. Mascal, M.; Hext, N. M.; Warmuth, R.; Arnall-Culliford, J. R.; Moore, M. H.; Turkenburg, J. P. *J. Org. Chem.* **1999**, *64*, 8479−8484. Marsh, A.; Silvestri, M.; Lehn, J.-M. *Chem. Commun.* **1996**, 1527−1528. Fenniri, H.; Deng, B.-L.; Ribbe, A. E. *J. Am. Chem. Soc.* **2002**, *124*, 11064−11072. Whitesides, G. M.; Simanek, E. E.; Mathias, J. P.; Seto, C. T.; Chin, D.; Mammen, M.; Gordon, D. M. *Acc. Chem. Res.* **1995**, *28*, 37−44.
(7) Vysotsky, M. O.; Thondorf, I.; Bohmer, V. *Angew. Chem., Int. Ed.* **2000**, *39*, 1264−1267.

chaperones.[18] The common strategy in the creation of these modules has been to increase the number and/or strength of the hydrogen bonds, reduce the number of unfavorable secondary interactions,[19] and tailor their geometrical arrangement. One disadvantage of this strategy is that the resulting aggregates often do not survive changes to H-bond competitive polar solvents.[20] In this paper, we employ a different strategy—conceptually related to Nolte's[21,22] use of molecular clips[23] as receptors for resorcinols and Gong's approach to backbone-rigidified folding oligomers[24]—that relies on a combination of $\pi-\pi$ interactions and hydrogen bonds. As $\pi-\pi$ interactions and hydrogen-bonding interactions show differential response to changes in solvent polarity, we hypothesized that these aggregates would display high stability over a broad range of solvents.

In a preliminary communication,[25] we showed that methylene-bridged glycoluril dimers **1** and **2**, bearing hydrogen-bonding functional groups on their aromatic rings, undergo tight dimerization in $CDCl_3$, form heterochiral dimers in highly diastereoselective recognition processes, and possess the ability to efficiently distinguish between self- and non-self forming complex self-sorted mixtures.[25,26] In this paper, we describe the dimerization characteristics of **1**−**8** in $CDCl_3$, demonstrate the stability and isostructural formation of **2·2** in solvents ranging from C_6D_6 to D_2O, and investigate the 21 binary mixtures comprising **1**−**7** for selective heterodimerization.

Results and Discussion

Synthesis of Compounds 1−8. The synthesis of **1**−**8** is shown in Scheme 1. Compound **9** was reduced to the corresponding air-sensitive diamine that was acylated with the appropriate acid chloride yielding **1**−**7** in good overall yield. To prepare **8**, we first alkylated **10** with **11** in DMSO using *t*-BuOK as base to yield a mixture of (±)-**12** and **13**. After chromatographic separation, **13** was reduced and then acylated with isonicotinoyl chloride to give **8** in 83% yield.

Compounds 1 and 2 Form Dimers in the Solid State. We were able to obtain single crystals of **1** and **2** from toluene and aqueous methanol, respectively. Figure 1 shows the structures of the dimers **1·1** and **2·2** determined by X-ray crystallography. The formation of dimer **1·1** is driven by a combination of $\pi-\pi$ interactions and two H-bonds.[27,28] In this head-to-head type geometry, the aromatic side-walls of one molecule of **1** fill the cleft of the opposing C-shaped molecule and vice versa. This geometry results in the display of the pendant benzoyl groups in a nearly collinear orientation on a single face of the dimer, a property that could be useful in the preparation of dynamic functional group arrays.[3,29] In contrast, the crystallization of **2** from aqueous methanol resulted in dimer **2·2** with different geometrical features. The formation of **2·2** is still driven by $\pi-\pi$ interactions, but no H-bonds between the two molecules of **2** are formed. In this head-to-tail type geometry, the pyridyl rings fill the cleft of the opposing C-shaped molecule and vice versa. We believe that crystal-packing forces are responsible for the observation of this alternate conformer in the solid state since **2·2** assumes a single conformation in a wide range of solvents (vide infra). Compounds **1** and **2**—and we hypothesize methylene-bridged glycoluril dimers in general—are able to interact with themselves via an ensemble of conformations via $\pi-\pi$ interactions between their aromatic rings. The selection of a single conformation from this ensemble of conformations occurs when the geometrical constraints of a second noncovalent interaction—in this case hydrogen bonds—are simultaneously imposed.

Compounds 1−6 and 8 Form H-bonded Dimers in $CDCl_3$ Solution. Significant anisotropic effects were observed in the ^1H NMR spectra recorded for **1**−**8** in $CDCl_3$ relative to DMSO-d_6, where **1**−**8** are monomeric (Figure 2). In particular, the

(8) Brunsveld, L.; Folmer, B. J. B.; Meijer, E. W.; Sijbesma, R. P. *Chem. Rev.* **2001**, *101*, 4071−4097. Zimmerman, S. C.; Zeng, F.; Reichert, D. E. C.; Kolotuchin, S. V. *Science* **1996**, *271*, 1095−1098. Ma, Y.; Kolotuchin, S. V.; Zimmerman, S. C. *J. Am. Chem. Soc.* **2002**, *124*, 13757−13769. Kim, Y.; Mayer, M. F.; Zimmerman, S. C. *Angew. Chem., Int. Ed.* **2003**, *42*, 1121−1126. Roy, S.; Rotello, V. M. *Acc. Chem. Res.* **2003**, *36*, 549−561. Rieth, L. R.; Eaton, R. F.; Coates, G. W. *Angew. Chem., Int. Ed.* **2001**, *40*, 2153-2156. Pollino, J. M.; Stubbs, L. P.; Weck, M. *J. Am. Chem. Soc.* **2004**, *126*, 563−567. Fogleman, E. A.; Yount, W. C.; Xu, J.; Craig, S. L. *Angew. Chem., Int. Ed.* **2002**, *41*, 4026−4028. Bushey, M. L.; Nguyen, T.-Q.; Nuckolls, C. *J. Am. Chem. Soc.* **2003**, *125*, 8264−8269. Castellano, R. K.; Rudkevich, D. M.; Rebek, J., Jr. *Proc. Natl. Acad. Sci. U.S.A.* **1997**, *94*, 7132−7137.

(9) Ishida, Y.; Aida, T. *J. Am. Chem. Soc.* **2002**, *124*, 10417−10419.

(10) Hof, F.; Craig, S. L.; Nuckolls, C.; Rebek, J., Jr. *Angew. Chem., Int. Ed.* **2002**, *41*, 1488−1508.

(11) Shivanyuk, A.; Rebek, J., Jr. *Angew. Chem., Int. Ed.* **2003**, *42*, 684−686.

(12) Hannessian, S.; Saladino, R.; Margarita, R.; Simard, M. *Chem. Eur. J.* **1999**, *5*, 2169−2183. Shi, X.; Fettinger, J. C.; Cai, M.; Davis, J. T. *Angew. Chem., Int. Ed.* **2000**, *39*, 3124−3127. Shi, X.; Fettinger, J. C.; Davis, J. T. *J. Am. Chem. Soc.* **2001**, *123*, 6738−6739. Marguly, E.; McDonald, R.; Branda, N. R. *Org. Lett.* **2000**, *2*, 3169−3172. Cooks, R. G.; Zhang, D.; Koch, K. J.; Gozzo, F. C.; Eberlin, M. N. *Anal. Chem.* **2001**, *73*, 3646−3655. Ten Cate, A. T.; Dankers, P. Y. W.; Kooijman, H.; Spek, A. L.; Sijbesma, R. P.; Meijer, E. W. *J. Am. Chem. Soc.* **2003**, *125*, 6860−6861. Chung, D. M.; Nowick, J. S. *J. Am. Chem. Soc.* **2004**, *126*, 3062−3063.

(13) Leigh, D. A.; Wong, J. K. Y.; Dehez, F.; Zerbetto, F. *Nature* **2003**, *424*, 174−179.

(14) Fernandez-Lopez, S.; Kim, H.-S.; Choi, E. C.; Delgado, M.; Granja, J. R.; Khasanov, A.; Kraehenbuehl, K.; Long, G.; Weinberger, D. A.; Wilcoxen, K. M.; Ghadiri, M. R. *Nature* **2001**, *412*, 452−456.

(15) Sakai, N.; Sorde, N.; Matile, S. *J. Am. Chem. Soc.* **2003**, *125*, 7776−7777.

(16) Nowick, J. S. *Acc. Chem. Res.* **1999**, *32*, 287−296.

(17) Kerckhoffs, J. M. C. A.; van Leeuwen, F. W. B.; Spek, A. L.; Kooijman, H.; Crego-Calama, M.; Reinhoudt, D. N. *Angew. Chem., Int. Ed.* **2003**, *42*, 5717−5722.

(18) Paraschiv, V.; Crego-Calama, M.; Ishi-i, T.; Padberg, C. J.; Timmerman, P.; Reinhoudt, D. N. *J. Am. Chem. Soc.* **2002**, *124*, 7638−7639.

(19) Pranata, J.; Wierschke, S. G.; Jorgensen, W. L. *J. Am. Chem. Soc.* **1991**, *113*, 2810−2819.

(20) Mammen, M.; Simanek, E. E.; Whitesides, G. M. *J. Am. Chem. Soc.* **1996**, *118*, 12614−12623.

(21) Sijbesma, R. P.; Kentgens, A. P. M.; Nolte, R. J. M. *J. Org. Chem.* **1991**, *56*, 3199−3201. Reek, J. N. H.; Priem, A. H.; Engelkamp, H.; Rowan, A. E.; Elemans, J. A. A. W.; Nolte, R. J. M. *J. Am. Chem. Soc.* **1997**, *119*, 9956−9964. Jansen, R. J.; Rowan, A. E.; de Gelder, R.; Scheeren, H. W.; Nolte, R. J. M. *Chem. Commun.* **1998**, 121−122. Jansen, R. J.; de Gelder, R.; Rowan, A. E.; Scheeren, H. W.; Nolte, R. J. M. *J. Org. Chem.* **2001**, *66*, 2643−2653.

(22) Reek, J. N. H.; Elemans, J. A. A. W.; Nolte, R. J. M. *J. Org. Chem.* **1997**, *62*, 2234−2243.

(23) Chen, C.-W.; Whitlock, H. W. *J. Am. Chem. Soc.* **1978**, *100*, 4921−4922. Rowan, A. E.; Elemans, J. A. A. W.; Nolte, R. J. M. *Acc. Chem. Res.* **1999**, *32*, 995−1006. Zimmerman, S. C. *Top. Curr. Chem.* **1993**, *165*, 71−102. Klarner, F.-G.; Kahlert, B. *Acc. Chem. Res.* **2003**, *36*, 919−932. Harmata, M.; Barnes, C. L.; Karra, S. R.; Elahmad, S. *J. Am. Chem. Soc.* **1994**, *116*, 8392−8393. Maitra, U.; Potluri, V. K. *J. Org. Chem.* **2000**, *65*, 7764−7769. Pardo, C.; Sesmilo, E.; Gutierrez-Puebla, E.; Monge, A.; Elguero, J.; Fruchier, A. *J. Org. Chem.* **2001**, *66*, 1607−1611.

(24) Gong, B.; Zeng, H.; Zhu, J.; Yuan, L.; Han, Y.; Cheng, S.; Furukawa, M.; Parra, R. D.; Kovalevsky, A. Y.; Mills, J. L.; Skrzypczak-Jankun, E.; Martinovic, S.; Smith, R. D.; Zheng, C.; Szyperski, T.; Zeng, X.-C. *Proc. Natl. Acad. Sci. U.S.A.* **2002**, *99*, 11583−11588. Yang, X.; Yuan, L.; Yamato, K.; Brown, A. L.; Feng, W.; Furukawa, M.; Zeng, X. C.; Gong, B. *J. Am. Chem. Soc.* **2004**, *126*, 3148−3162.

(25) Wu, A.; Chakraborty, A.; Fettinger, J. C.; Flowers, R. A., II; Isaacs, L. *Angew. Chem., Int. Ed.* **2002**, *41*, 4028−4031.

(26) Wu, A.; Isaacs, L. *J. Am. Chem. Soc.* **2003**, *125*, 4831−4835. Mukhopadhyay, P.; Wu, A.; Isaacs, L. *J. Org. Chem.* **2004**, *69*, ASAP.

(27) For a review of H-bond geometry, see: Taylor, R.; Kennard, O. *Acc. Chem. Res.* **1984**, *17*, 320−326.

(28) For **1·1**, the two external amide protons are strongly H-bonded to the internal amide C=O groups with normal bond distances (N···O = 2.937 Å, H···O = 2.088 Å) and angles (N−H···O = 162.0°), whereas the structural data indicate that the internal amide N−H groups may benefit from weaker interactions with the ureidyl C=O groups (N···O = 2.909 Å, H···O = 2.240 Å, and N−H···O = 132.6°).

(29) Lehn, J.-M.; Eliseev, A. V. *Science* **2001**, *291*, 2331−2332.

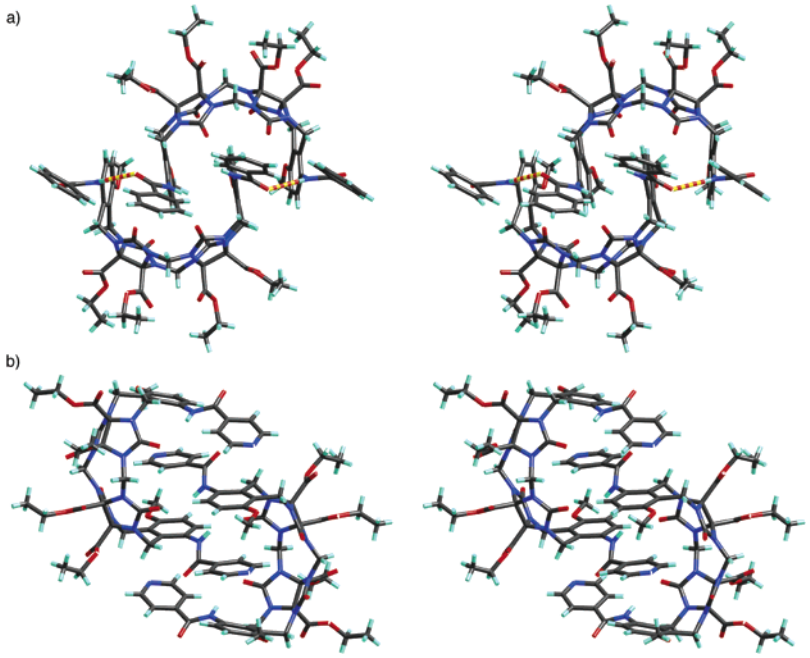

Figure 1. Stereoviews of the molecular structures of (a) **1·1**, and (b) **2·2** in the crystal. Solvating CH_3OH, H_2O, and $PhCH_3$ have been removed for clarity. Some of the CO_2Et groups adopt two orientations in the crystal; here, the major orientation component is depicted. C, gray; H, green; N, blue; O, red; and H-bonds, yellow-red striped.

Scheme 1

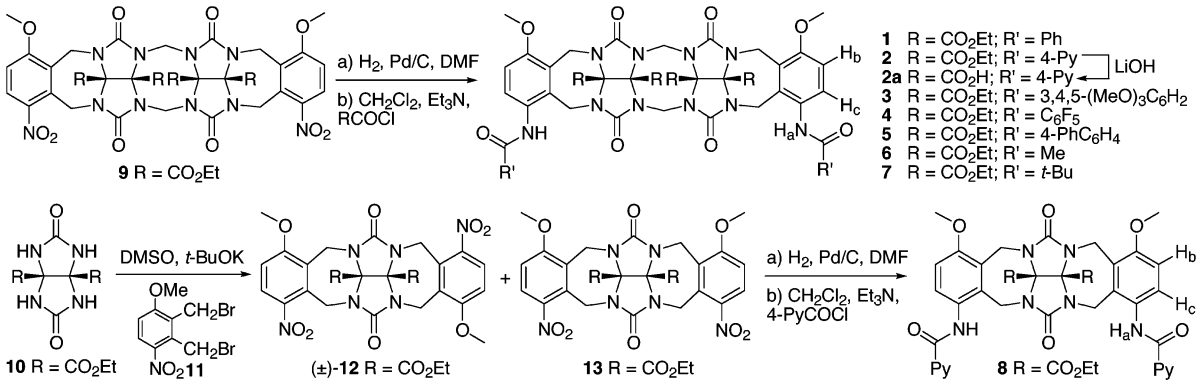

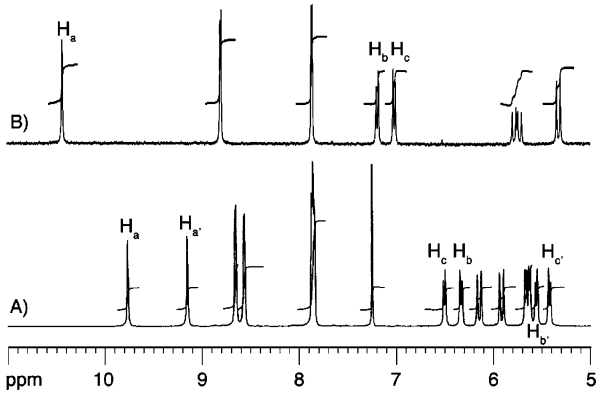

Figure 2. Portion of the ^1H NMR spectrum recorded for **2·2** (400 MHz, room temperature) in (A) $CDCl_3$ and (B) DMSO-d_6.

chemical shifts observed for H_a and $H_{a'}$ suggested the presence of N−H···O hydrogen-bonding interactions whereas the strong upfield shifts experienced by H_b and H_c indicated the proximity of these protons to the shielding region of a neighboring aromatic ring (Table 1). The observed doubling of resonances for H_a−H_c further suggested the presence of monomer−dimer equilibrium in solution, with a dimer geometry containing well-defined external (Ar_{out}, H_a−H_c) and internal (Ar_{in}, $H_{a'}$−$H_{c'}$) aromatic rings.[25,30,31] Figure 1a shows a stereoview of the geometry of **1·1** in the solid state determined by X-ray crystallography. The solid-state geometry of **1·1** is fully consistent with the features of the NMR spectra of **1·1** described above, and we suggest that **1·1** is isostructural in solution and the solid state.

Further evidence for the presence of a monomer−dimer equilibrium comes from several sources (Table 1). First, the molecular weights of **1**−**6** and **8** determined by GPC in chloroform lie between those of the monomer and the dimer. Second, the observation of cross-peaks in the EXSY spectrum

(30) Reek, J. N. H.; Kros, A.; Nolte, R. J. M. *Chem. Commun.* **1996**, 245−246. Elemans, J. A. A. W.; de Gelder, R.; Rowan, A. E.; Nolte, R. J. M. *Chem. Commun.* **1998**, 1553−1554. Elemans, J. A. A. W.; Slangen, R. R. J.; Rowan, A. E.; Nolte, R. J. M. *J. Inclusion Phenom. Macrocyclic Chem.* **2001**, *41*, 65−68. Elemans, J. A. A. W.; Rowan, A. E.; Nolte, R. J. M. *J. Am. Chem. Soc.* **2002**, *124*, 1532−1540. Elemans, J. A. A. W.; Slangen, R. R. J.; Rowan, A. E.; Nolte, R. J. M. *J. Org. Chem.* **2003**, *68*, 9040−9049. Isaacs, L.; Witt, D.; Lagona, J. *Org. Lett.* **2001**, *3*, 3221−3224. Isaacs, L.; Witt, D. *Angew. Chem., Int. Ed.* **2002**, *41*, 1905−1907.
(31) Reek, J. N. H.; Elemans, J. A. A. W.; de Gelder, R.; Beurskens, P. T.; Rowan, A. E.; Nolte, R. J. M. *Tetrahedron* **2003**, *59*, 175−185.

Table 1. Selected ^{1}H NMR, EXSY, K_s (400 MHz, $CDCl_3$, 298 K, 10 MM), and GPC Data for **1**−**8**

	δ NH		δ Ar_{out}[c]		δ Ar_{in}[c]			MW		
compound	H_a	$H_{a'}$	H_b	H_c	$H_{b'}$	$H_{c'}$	k_{ex} (s^{-1})	calcd	GPC	K_s M^{-1}
1	9.79	8.97	6.29	6.45	5.53	5.43	14	1099	1523	$> 9 \times 10^5$
2	9.76	9.13	6.32	6.50	5.54	5.41	6	1101	1303	$> 9 \times 10^5$
3	9.77	9.00	6.40	6.50		5.43	20	1279	1947	$> 9 \times 10^5$
4	9.19	8.80		6.47	5.50	5.32	4	1279	1629	$> 9 \times 10^5$
5	9.84	9.10	6.32	6.55	5.59	5.49	5	1251	1781	$> 9 \times 10^5$
6	9.10	8.27		6.31	5.36	5.14	7	975	1904	$> 9 \times 10^5$
7[a]	8.45				6.79	7.38		1059	1043	
8[b]	10.44	10.10	6.45	6.62	5.60	5.45		820	653	920 ± 50

[a] Compound **7** is monomeric in $CDCl_3$; accordingly, only one set of resonances for H_a−H_c are reported. [b] Recorded at −50 °C ([**8**] = 1 mM). [c] Assignments are based on cross peaks observed in the COSY and ROESY spectra.

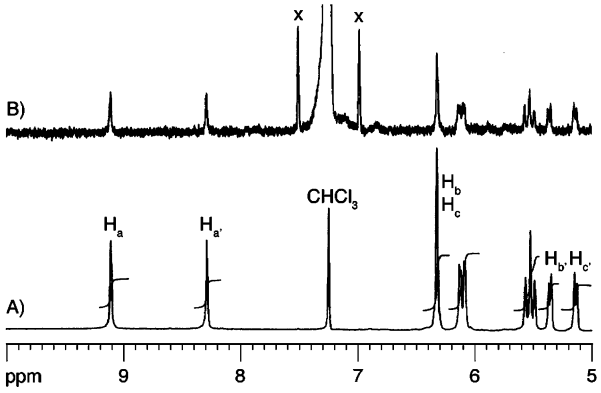

Figure 3. Portion of the ^{1}H NMR spectrum recorded for **6·6** (400 MHz, room temperature) in $CDCl_3$ at (A) 10 mM and (B) 50 μM. x = $^{13}CHCl_3$.

confirmed the slow chemical exchange between the interior and exterior of the aggregate and allowed calculation of the corresponding values of the exchange rate constant (k_{ex}, Table 1).[32] Third, we observe a single type of heterodimer when two different molecular clips are mixed *(*vide infra*)*.[25] Last, X-ray crystallography of methylene-bridged glycoluril dimers (vide supra) has consistently yielded dimers.[25] Compound **7**, with its bulky *t*-Bu groups, remains monomeric in $CDCl_3$ solution.

The preceding sections establish that **1**−**6** and **8** undergo dimerization in $CDCl_3$ solution. In an attempt to determine the values of the self-association constant (K_s) for **1**−**6** and **8**, we performed ^{1}H NMR dilution experiments. Remarkably, the chemical shifts observed for the dimeric forms of **1**−**6** do not respond to changes in concentration between 10 mM and 50 μM, indicating remarkably high thermodynamic stability (Figure 3). If we assume that we could detect changes in chemical shift due to the presence of 10% monomer, then we can place a lower limit on the value of K_s ($K_s > 9 \times 10^5$ M^{-1}, $-\Delta G > 8.1$ kcal mol^{-1}). We hypothesized that the high thermodynamic stability observed for **1·1** and **2·2** was due to favorable $\pi-\pi$ interactions between their *o*-xylylene rings, whose tips are pinched only slightly inward from coplanarity at a distance (7.4 and 7.6 Å).[25,33] Accordingly, we compared the behavior of **1**−**6** with **8**, which contains a single glycoluril ring. Nolte has demonstrated that such compounds assume a geometry where the tips of the *o*-xylylene rings are splayed slightly outward;[34] molecular modeling of **8·8** (MMFF) indicates a separation of 7.4 Å. In contrast to the behavior of **2**, **8** displays a single set of ^{1}H NMR resonances whose chemical shifts are concentration-dependent at room temperature. This behavior indicates a fast monomer−dimer equilibrium on the chemical-shift time scale whose value of K_s could be determined by fitting the changes in chemical shift as a function of concentration ($K_s = 920 \pm 50$ M^{-1}). The difference between the stability of dimers **2·2** and **8·8** ($\Delta\Delta G > 4.1$ kcal mol^{-1}) is surprisingly large. Examination of the structures of **2·2** and **8·8** suggests that the geometrical requirements of the $\pi-\pi$ interactions and H-bonds are more commensurate within **2·2** than for **8·8**.

Dimeric Aggregates 1·1−6·6 Are Isostructural in $CDCl_3$. Because of their proximity to the neighboring aromatic rings in the dimeric aggregate, the *o*-xylylene protons (H_a−H_c) are sensitive indicators of aggregate geometry. These protons resonate at remarkably constant chemical shifts (H_b, 6.35 ± 0.07; H_c, 6.46 ± 0.11; $H_{b'}$, 5.49 ± 0.08; and $H_{c'}$, 5.37 ± 0.13) in aggregates **1·1**−**6·6**, bearing a range of acyl groups (Table 1). Accordingly, **1·1**−**6·6** assume a common geometry in $CDCl_3$ solution. We do not consider the chemical shift of the amide NH_a groups since they are influenced by the electronic nature of the acyl substituents.

Compound 2 Forms Tightly Associated Isostructural Dimers Across the Full Range of Solvents. Solvent typically plays a dominant role in the outcome of molecular-recognition and self-assembly studies. For example, hydrophobically driven binding within cyclophanes is a linear function of solvent polarity ($E_T(30)$).[35] Conversely, aggregates driven by the formation of hydrogen bonds are less stable in more-polar solvents containing hydrogen bond donor and/or acceptor functional groups.[20] Given the opposing solvent dependence of the strength of $\pi-\pi$ interactions and H-bonds, the apparent high level of cooperativity between the $\pi-\pi$ interactions and H-bonds in the formation of **2·2**, and the fact that only a single conformer of **2·2** simultaneously satisfies the geometrical requirements of both the π-π interactions and H-bonds we wondered how **2·2** would respond to changes in solvent. We hypothesized that **2·2** would display a high thermodynamic stability across the full range of solvents, that is, the H-bonds would provide the main but not exclusive driving force in nonpolar media, whereas the $\pi-\pi$ interactions would provide the main but not exclusive driving force in more polar, protic solvents.[28,36] We further hypothesized

(32) Perrin, C. L.; Dwyer, T. J. *Chem. Rev.* **1990**, *90*, 935−967.
(33) Wu, A.; Chakraborty, A.; Witt, D.; Lagona, J.; Damkaci, F.; Ofori, M.; Chiles, K.; Fettinger, J. C.; Isaacs, L. *J. Org. Chem.* **2002**, *67*, 5817−5830.
(34) Sijbesma, R. P.; Kentgens, A. P. M.; Lutz, E. T. G.; van der Maas, J. H.; Nolte, R. J. M. *J. Am. Chem. Soc.* **1993**, *115*, 8999−9005.
(35) Smithrud, D. B.; Diederich, F. *J. Am. Chem. Soc.* **1990**, *112*, 339−343.
(36) The driving force for the formation of **2·2** in nonpolar solvents cannot be attributed solely to the formation of two H-bonds given the large value of K_s ($> 9 \times 10^5$ M^{-1}); weaker electrostatic interactions and $\pi-\pi$ interactions are also involved. Conversely, in polar protic solvents, $\pi-\pi$ interactions play a primary role and the H-bonds are of secondary importance.

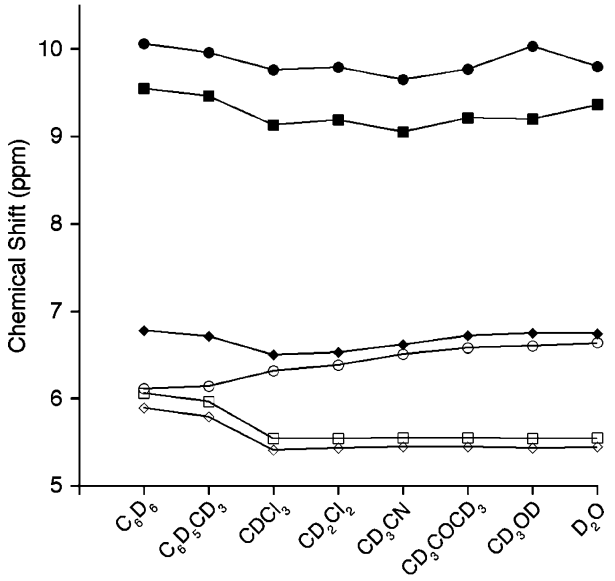

Figure 4. Chemical shifts observed for **2·2** (H_a, ●; $H_{a'}$, ■; H_c, ♦; H_b, ○; $H_{b'}$, □; and $H_{c'}$, ◊) as a function of solvent.

that such an aggregate would be isostructural across the full range of solvents, that is, the dimer **2·2** would assume a single geometry.

The data shown in Figure 4 provide some experimental support for these hypotheses. For example, the values of K_s are large in nonpolar solvents ($CDCl_3$, $> 9 \times 10^5$ M^{-1}; $C_6D_5CD_3$, $> 9 \times 10^5$ M^{-1}; and C_6D_6, $> 9 \times 10^5$ M^{-1}) and in polar, protic solvents (CD_3OD, $> 9 \times 10^5$ M^{-1} and D_2O, 36300 M^{-1}). In solvents of intermediate polarity containing H-bond-accepting functional groups (CD_3CN, 3350 M^{-1}; CD_3COCD_3, 20300 M^{-1}; and CD_3SOCD_3, no detectable self-assocation), the values of K_s are reduced. We attribute this decrease in K_s to the ability of these solvents to act as competitive hydrogen-bond acceptors while not providing a significant hydrophobic driving force. Superimposed on the general trends are effects that can be attributed to specific solvation. For example, in CD_2Cl_2, the self-association constant is low ($K_s = 5700$ M^{-1}) and the rates of dynamic exchange processes within **2·2** are higher than in $CDCl_3$ that necessitated working at −30 °C to achieve slow exchange on the chemical-shift time scale. Similarly, we have previously observed the ability of CH_3CN to fill the cleft of methylene-bridged glycoluril dimers[33] and attribute the relatively low value of K_s observed in CD_3CN to a specific solvation effect. In CD_3SOCD_3, a highly competitive H-bond-accepting solvent that does not promote solvophobically driven complexation, **2** remains monomeric. Even more striking than the relatively high stability of **2·2** across a wide range of solvents is the remarkable constancy of the chemical shifts observed for H_a-H_c and $H_{a'}-H_{c'}$ (Figure 4). The chemical shift of protons on the *o*-xylylene rings of **2** are highly sensitive indicators of their orientation (distance and angle) relative to the mean plane defined by the aromatic carbon atoms.[37] Similarly, the chemical shift of H_a and $H_{a'}$ will be sensitive to the degree of H-bonding. Taken together, the similarity of the chemical shifts observed for H_a-H_c and $H_{a'}-H_{c'}$ suggests that the dimeric complex **2·2** assumes a common geometry across the full range of solvents.

Mixtures of Compounds 1−8 Form Homodimers and Heterodimers. How does the ability of **2·2** to assume a single conformation across a wide range of solvents endow it with properties that exceed or are at least different than those of a simple rigid molecule (e.g., naphthalene) or a foldamer[24] that is also isostructural? One answer lies in the fact that the dimerization of **1**−**6** and **8** are bimolecular processes, whereas folding is an inherently unimolecular process. Therefore, even though these dimers are isostructural, they are capable of responding to the presence of other methylene-bridged glycoluril dimers in their environment to form heterodimers. The collinear orientation of amide substituents (Figure 1a) in these dimers means that homodimers and heterodimers present vastly different molecular surfaces for potential recognition processes. We wanted to determine, therefore, whether the steric or electronic nature of the amide substituent could be used to dictate the selective formation of either homodimer or heterodimer.[7,38] Equations 1 and 2 define the equilibrium between homodimers (AA and BB) and heterodimer AB. When the total concentrations of A and B are equal, a statisical mixture comprises half homodimer (25% AA and 25% BB) and half heterodimer. As such, the equilibrium constant for a statistical mixture is equal to 4. Equilibrium constants less than 4 represent a preference for the homodimeric forms, whereas values greater than 4 represent a preference for the heterodimer. Because of the quadratic form of K_{eq}, we also define the mole fraction of heterodimer (χ_{AB}) as given in eq 3. When [AA] = [BB], eq 3 can be readily manipulated to yield eq 4. Equation 4 demonstrates that χ_{AB} depends on $\sqrt{K_{eq}}$, rather than the more usual dependence on K_{eq}, and provides a rationale for the high values of K_{eq} needed to achieve selective heterodimer formation. Table 2 gives the parameters governing the 21 different heterodimeric pairs comprising **1**−**7**. Despite the range of amide substituents, the percentage of heterodimer remains in the quite modestly selective range (30−70%) for 16 out of the 21 pairs measured. The most selective pair, comprising a mixture of **4** and **6** bearing pentafluorophenyl and methyl substituents, results in heterodimer formation with $\chi_{\mathbf{4\cdot6}} = 0.933$.[39] Figure 5 shows the ^{1}H NMR spectra recorded for **4**, **6**, and an equimolar mixture of **4** and **6**. The highly heterodimer-selective process is not easily rationalized given the steric similarity of **4** and **1**, **2**, and **3** and the electronic similarity of **6** and **7**, which all show modest levels of selectivity when paired with **4** or **6**, respectively.[40] All of the other relatively selective pairs—homodimeric and heterodimeric—involve molecular clip **7**, which is monomeric in $CDCl_3$. Mixtures of **7** and **2** and **7** and **6** form heterodimers **7·2** and **7·6** selectively, whereas mixtures of **7** and **3** and **7** and **5** selectively form homodimers **3·3** and **5·5**, along with monomeric **7**. Given that these mixtures have reached thermodynamic equilibrium, the driving force for these selective homo- and heterodimerization processes must be a minimization of free energy.

(37) Johnson, C. E.; Bovey, F. A. *J. Chem. Phys.* **1958**, *29*, 1012−1014. Emsley, J. W.; Feeney, J.; Sutcliffe, L. H. *High-Resolution Nuclear Magnetic Resonance Spectroscopy*; Pergamon Press: New York, 1965; Vol. 1.

(38) Castellano, R. K.; Rebek, J., Jr. *J. Am. Chem. Soc.* **1998**, *120*, 3657−3663.

(39) To investigate the influence of solvation on the heterodimerization process, we determined the values of the heterodimerization equilibrium constant, K_{eq}, and $\chi_{\mathbf{4\cdot6}}$ for an equimolar mixture of **4** and **6** as a function of solvent: $CDCl_3$ ($K_{eq} = 768$, $\chi_{\mathbf{4\cdot6}} = 0.933$), CD_2Cl_2 (840, 0.935), C_6D_6 (608, 0.925), $C_6D_5CD_3$ (762, 0.932), CD_3COCD_3 (552, 0.922), CD_3CN (351, 0.904), and CD_3OH (694, 0.929). Solvation does not appear to play an important role in the highly selective heterodimerization process observed for **4·6**.

(40) We have performed simple force field calculations (Spartan 02, MMFF) for **4·4**, **6·6**, and **4·6**. We do not observe any major differences between the three structures that might explain this highly heterodimer selective process.

Table 2. Dimensionless Equilibrium Constants, K_{eq}, and Heterodimer Mole Fractions (χ_{AB}) for Binary Mixtures of **1**−**7**

components R′	**2**	**3**	**4**	**5**	**6**	**7** *t*-Bu
1 Ph	21.72 (70.0)	14.5 (65.5)	3.44 (48.1)	9.36 (60.3)	3.2 (47.2)	1.28 (36.1)[a]
2 4-Py		13.7 (64.9)	11.1 (62.5)	6.44 (55.9)	9.84 (61.0)	275 (89.2)
3 $(MeO)_3C_6H_2$			3.36 (47.6)	3.84 (49.4)	9.64 (60.8)	0.23 (25.3)[a]
4 C_6F_5				1.04 (33.9)	768 (93.3)	1.04 (33.8)[a]
5 4-PhC_6H_4					1.8 (40.1)	0.58 (26.4)[a]
6 Me						31.9 (73.8)
						333 (90.1)[a]

[a] Recorded at −55 °C.

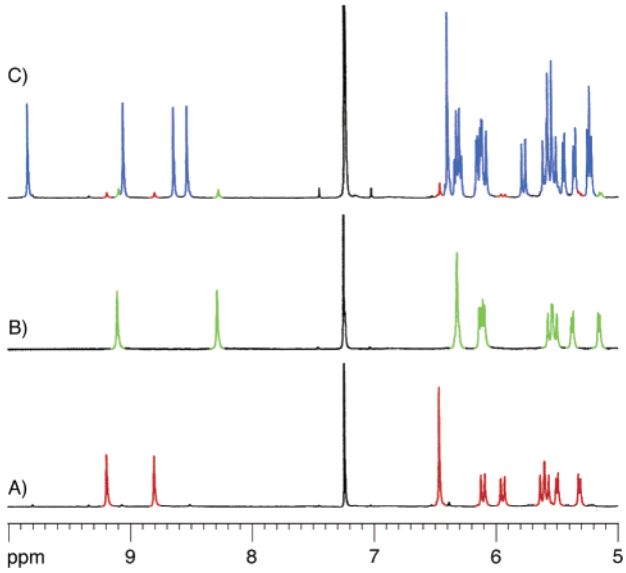

Figure 5. Portion of the ^{1}H NMR spectrum recorded (1 mM, $CDCl_3$, 400 MHz, room temperature) for (A) **4·4**, (B) **6·6**, and (C) a mixture of **4·4**, **6·6**, and **4·6**. Resonances are color coded as follows: **4·4**, red; **6·6**, green; **4·6**, blue.

$$AA + BB \overset{K_{eq}}{\rightleftharpoons} 2\ AB \quad (1)$$

$$K_{eq} = [AB]^2/[AA][BB] \quad (2)$$

$$\chi_{AB} = [AB]/([AA] + [AB] + [BB]) \quad (3)$$

$$\chi_{AB} = \sqrt{K_{eq}}/(\sqrt{K_{eq}} + 2) \quad (4)$$

To explore the preference of **7** to engage in selective homodimerization or heterodimerization, we performed the simulation shown in Figure 6 comprising two components (A and B) that are capable of forming dimers AA, BB, and AB. We fix the total concentrations of A and B ($[A_{tot}] = [B_{tot}] = 1$ mM) and the values of K_{AA} and K_{BB} (0 and 10^6 M^{-1}) to simulate the behavior of **7** and **1**−**6**. When the value of K_{AB} is low ($<10^3$ M^{-1}), homodimer BB and monomeric A are formed in a highly selective process. Similarly, when K_{AB} is high ($>10^6$ M^{-1}), heterodimer AB is formed selectively ($\chi_{AB} > 0.88$). Somewhat surprisingly, the value of K_{AB} ($\approx 10^5$ M^{-1}) needed to achieve a statistical mixture ($\chi_{AB} = 0.5$) is *10-fold less* than the fixed value of K_{BB} (10^6 M^{-1}).[41] As the difference between the fixed values of K_{AA} and K_{BB} increases, so does the difference between the values of K_{AB} and K_{BB} needed to achieve a statistical mixture. The reason is simple but instructive; the free energy gained by

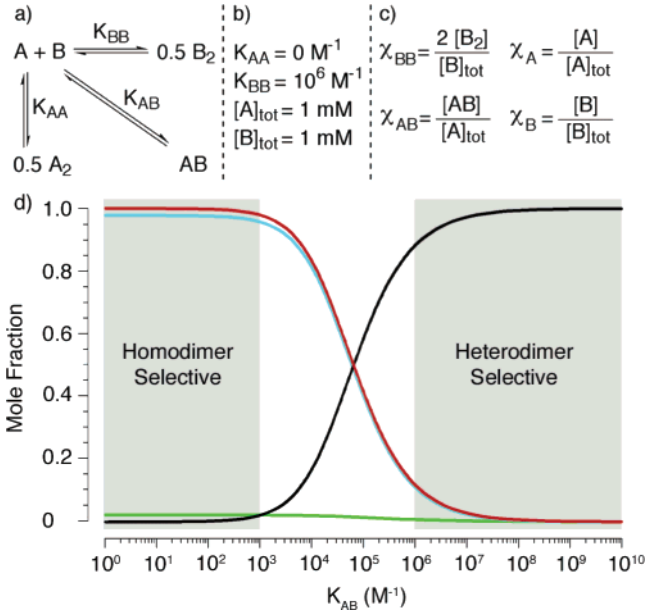

Figure 6. Mole fraction values depend on the relative value of K_{AB}: (a) equilibria considered, (b) constraints imposed, (c) mole fraction definitions, and (d) a plot of mole fraction versus K_{AB}. Legend: χ_A, red; χ_{BB}, aqua; χ^g_{AB}, black; and χ_B, green.

conversion of AA (or A) into AB may be used to pay for the loss in free energy due to the transformation of BB into AB. It is not necessary for the heterodimerization equilibrium constant (K_{AB}) to exceed the values of the homodimerization equilibrium constants (K_{AA} and K_{BB}) for a heterodimerization-selective process to occur as long as the difference between K_{AA} and K_{BB} is large. Such appears to be the case for mixtures comprising **7** and **2** or **6**.[42] The level of homodimer selectivity ($\chi_{AB} \approx 0.25$) obtained for mixtures of **7** and **3** or **5** requires a value of $K_{AB} = 2 \times 10^4$ M^{-1} using the constraints imposed in Figure 6.

Conclusions

In summary, we have presented the synthesis and self-association properties of molecular clips **1**−**8**, which bear two H-bonding amide substituents on their aromatic rings. Compounds **1**−**6** form tight dimers in $CDCl_3$ ($K_s > 9 \times 10^5$ M^{-1}), whereas **8** is more than 1000-fold less strongly dimerized ($K_s = 920 \pm 50$ M^{-1}), which demonstrates the importance of the methylene-bridged glycoluril dimer skeleton compared to molecular clips shaped by a single glycoluril ring.[31] The differential response of the strength of the H-bonds and $\pi-\pi$ interactions

(41) Grote, Z.; Scopelliti, R.; Severin, K. *Angew. Chem., Int. Ed.* **2003**, *42*, 3821−3825.

(42) This explanation could also rationalize the observed highly heterodimer-selective formation of **4·6** if one of the homodimeric assemblies (**4·4** or **6·6**) was significantly less stable than the other. Indeed, we have seen indications that **4·4** may be less stable than homodimers formed from **1**−**3**, **5**, and **6**.

driving the formation of **2·2** confers moderate to high stability in solvents ranging from C_6D_6 to D_2O, although specific solvation effects can also be discerned. Aggregate **2·2** is isostructural—that is it assumes a common geometry—across the full range of solvents, as judged by the relative solvent independence of diagnostic chemical shifts (H_a, H_b, and H_c). Last, binary mixtures of **1**−**7** result in the formation of homodimers and heterodimers with moderate levels of selectivity ($0.253 < \chi_{AB} < 0.933$).

The results of this study demonstrate a number of principles of potentially broad applicability. First, employing tactical combinations of $\pi-\pi$ interactions and a small number of H-bonds[21] is a practical alternative to the common strategy of simply increasing the number of H-bonds to improve the stability of H-bonded aggregates. Second, by employing a relatively rigid building block, in this case methylene-bridged glycoluril dimers, it is possible to limit the range of $\pi-\pi$ stacked dimeric geometries to a well-defined ensemble. By simultaneously employing a second orthogonal noncovalent interaction, in this case hydrogen bonds, it is possible to reliably select a single dimer geometry from this molecular ensemble. Third, employing two noncovalent interactions ($\pi-\pi$ interactions and H-bonds) whose strengths respond differently to changes in solvent results in a solvent-independent isostructural aggregate. Aggregates that are isostructural across a range of solvents possess significant potential as components of instructed supramolecular systems. The behavior of such structurally invariant components[24] complements that of known systems whose geometries are responsive to changes in solvent.[5] Fourth, simulations of the behavior of **7** and **1**−**6** demonstrate a strategy for the selective formation of heterodimers—namely maximization of the difference between K_{AA} and K_{BB} while maintaining a moderate value of K_{AB}.

Previously, we reported that **1**, **2**, and congeners possess a confluence of properties—tight dimerization, highly diastereoselective (heterochiral) recognition processes, and self-sorting—that make them prime modules for use in advanced applications. Here, we extend this range of properties to include tight dimerization across the full range of solvents while the aggregates remain isostructural. We believe that aggregates that possess such a wide range of properties will become important components in complex adaptive self-sorting systems.[4,25,26]

Experimental Section

General. Starting materials were purchased from commercial suppliers and were used without further purification. Compounds **1**, **2**, **9**, **10**, and **11** were prepared according to literature procedures.[25,33] THF and toluene were distilled from sodium benzophenone ketyl, and methylene chloride was distilled from CaH_2 immediately before use. TLC analysis was performed using precoated plates from E. Merck. Column chromatography was performed using silica gel (230−400 mesh, 0.040−0.063 μm) from E. Merck using eluents in the indicated v:v ratio. Melting points were measured on a Meltemp apparatus in open capillary tubes and are uncorrected. IR spectra were recorded on a Nicolet Magna spectrophotometer as KBr pellets or thin films on NaCl plates and are reported in cm^{-1}. NMR spectra were measured on Bruker AM-400, DRX-400, and DMX-500 instruments, operating at 400 or 500 MHz for ^1H and 100 or 125 MHz for ^{13}C. Mass spectrometry was performed using a VG 7070E magnetic sector instrument by electron impact (EI) or by fast atom bombardment (FAB) using the indicated matrix. The matrix "magic bullet" is a 5:1 (w:w) mixture of dithiothreitol:dithioerythritol. Elemental analyses were performed by Midwest MicroLab (Indianapolis, IN).

Compound 2a. A mixture of **2** (110 mg, 0.10 mmol) and LiOH (24 mg, 1.0 mmol) was suspended in a mixture of MeOH (30 mL) and water (30 mL). The resulting suspension was heated at 70 °C for 40 h. The reaction mixture was concentrated, dissolved in a minimum amount of H_2O, and neutralized with $HClO_4$ (0.105 mL, 1.22 mmol). The suspension was centrifuged, the supernatant pipetted off, and the residue was washed with water (3 × 0.5 mL). After being dried at high vacuum, an aqueous solution of **2a** was lyophilized to give **2a** as a fluffy solid (77.2 mg, 0.065 mmol, 64%). Mp > 300 °C (dec). IR (KBr, cm^{-1}) 3445m, 1718s, 1662s, 1539m, 1487m, 1466m, 1366m, 1277s, 914m. ^1H NMR (400 MHz, DMSO-d_6) 10.40 (s, 2H), 8.81 (br. m, 4H), 7.88 (br. m, 4H), 7.13 (br., 2H), 6.97 (br., 2H), 5.65 (d, J = 15.6, 1H), 5.60 (d, J = 15.8, 1H), 5.44 (d, J = 16.1, 2H), 4.85−4.80 (m, 3H), 4.67 (d, J = 15.6 Hz, 1H), 4.15−3.90 (m, 4H), 3.70 (s, 6H) ppm. ^{13}C NMR (100 MHz, TFA) 171.3, 168.4, 166.8, 160.1, 159.9, 152.5, 144.9, 134.7, 131.5, 128.7, 127.1, 126.2, 114.6, 83.3, 83.0, 57.3, 50.6, 42.2, 39.7 ppm (only 19 of the 21 expected resonances were observed). MS (FAB, Magic Bullet) m/z 989 (100, $[M + H]^+$). HR-MS (FAB, Magic Bullet) m/z 989.2468 ($[M + H]^+$, $C_{44}H_{37}N_{12}O_{16}$, calcd 989.2450). Anal. calcd for $C_{44}H_{37}ClN_{12}O_{20}$ (1089.29), C 48.52, H 3.42. Found, C 48.31, H 3.99.

Compound 3. A mixture of **9** (72 mg, 0.076 mmol) and 10% Pd/C (50 mg) in anhydrous DMF (10 mL) was stirred under H_2 (10−20 psi) at room temperature for 5 h. The reaction mixture was filtered under Ar and concentrated under high vacuum at room temperature. The residue was dissolved in a mixture of anhydrous degassed CH_2Cl_2 (10 mL) and NEt_3 (0.5 mL, 4 mmol). This solution was added to a solution of 3,4,5-trimethoxybenzoyl chloride (70 mg, 0.30 mmol) in anhydrous degassed CH_2Cl_2 (5 mL) at −78 °C. After 15 min, the cooling bath was removed, and stirring was continued at room temperature for 12 h. The reaction mixture was diluted with $CHCl_3$ (100 mL), washed with saturated aqueous $NaHCO_3$, dried over anhydrous $MgSO_4$, and concentrated. Flash chromatography (SiO_2, $CHCl_3$/MeOH, 50:1) gave **3** (95 mg, 0.074 mmol, 98%). Mp > 300 °C (dec). TLC ($CHCl_3$/MeOH 10:1) R_f 0.55. IR (KBr, cm^{-1}) 3257w, 2940w, 2848w, 1747s, 1653m, 1585m, 1488m, 1456m, 1369m, 1335s, 1278s, 1253s, 1128m, 1084m, 1018m, 909m. ^1H NMR (400 MHz, DMSO-d_6) 9.93 (br. s, 2H), 7.29 (s, 4H), 7.14 (br. m, 2H), 6.95 (br. m, 4H), 5.76 (d, J = 16.0 Hz, 1H), 5.70 (d, J = 16.1 Hz, 1H), 5.28 (d, J = 15.9 Hz, 2H), 4.76 (d, J = 16.2 Hz, 2H), 4.53 (d, J = 16.0 Hz, 1H), 4.42 (d, J = 16.1 Hz, 1H), 4.30−4.00 (m, 12H), 3.86 (s, 12H), 3.81 (s, 6H), 3.70 (s, 6H), 1.25−1.10 (m, 12H) ppm. ^{13}C NMR (100 MHz, DMSO-d_6) 165.3, 164.9, 163.9, 154.7, 154.5, 154.0, 152.7, 140.4, 133.7, 129.1, 128.6, 127.2, 124.9, 111.6, 105.2, 79.9, 78.6, 64.4, 63.8, 60.1, 56.2, 56.0, 47.4, 47.3, 36.2, 13.6, 13.5 ppm (only 27 of the 28 expected resonances were observed). MS (FAB, Magic Bullet) m/z 1279 (6, $[M + H]^+$), 135 (100). HR-MS (FAB, Magic Bullet) m/z 1411.3450 ($[M + Cs]^+$, $C_{60}H_{66}N_{10}O_{22}$-Cs, calcd 1411.3407).

Compound 4. A mixture of **9** (62 mg, 0.065 mmol) and 10% Pd/C (60 mg) in anhydrous DMF (10 mL) was stirred under H_2 (10−20 psi) at room temperature for 5 h. The reaction mixture was filtered under Ar and concentrated under high vacuum at room temperature. The residue was dissolved in a mixture of anhydrous degassed CH_2Cl_2 (10 mL) and NEt_3 (0.5 mL, 4 mmol). This solution was added to a solution of pentafluorobenzoyl chloride (33 mg, 0.14 mmol) in anhydrous degassed CH_2Cl_2 (5 mL) at −78 °C. After 15 min, the cooling bath was removed and stirring was continued at room temperature for 4 h. The reaction mixture was diluted with $CHCl_3$ (100 mL), washed with saturated aqueous $NaHCO_3$, dried over anhydrous $MgSO_4$, and concentrated. Flash chromatography (SiO_2, $CHCl_3$/MeOH, 50:1) gave **4** (95 mg, 0.074 mmol, 98%). Mp > 300 °C (dec). TLC ($CHCl_3$/MeOH 25:1) R_f 0.29. IR (KBr, cm^{-1}) 3245w, 2987w, 1751s, 1673m, 1600w, 1505s, 1456s, 1370m, 1260s, 1177w, 1084m, 1020s, 909s. ^1H NMR (400 MHz, DMSO-d_6) 10.66 (s, 2H), 7.07 (d, J = 8.8 Hz, 2H), 6.97

(d, J = 8.8 Hz, 2H), 5.76 (d, J = 16.1 Hz, 1H), 5.74 (d, J = 16.1 Hz, 1H), 5.24 (d, J = 15.7 Hz, 2H), 4.84 (d, J = 16.0 Hz, 2H), 4.50 (d, J = 16.1 Hz, 1H), 4.40 (d, J = 16.1 Hz, 1H), 4.35−4.00 (m, 12H), 3.76 (s, 6H), 1.21 (t, J = 7.1 Hz, 1H), 1.14 (t, J = 7.1 Hz, 6H). ^{13}C NMR (100 MHz, $CDCl_3$) 164.0, 156.4, 155.3, 154.1 ($^3J_{CF}$ = 18 Hz), 143.2 ($^1J_{CF}$ = 249 Hz), 141.3 ($^1J_{CF}$ = 254 Hz), 136.9 ($^1J_{CF}$ = 251 Hz), 134.0, 127.4, 126.6, 124.9, 112.2 ($^2J_{CF}$ = 21 Hz), 111.9, 79.8, 78.5, 64.4, 63.8, 56.2, 47.3, 47.2, 36.1, 13.54, 13.50 ppm (only 24 of the 26 expected resonances were observed). MS (FAB, Magic Bullet) m/z 1279 (75, $[M + H]^+$), 195 (100). HR-MS (FAB, Magic Bullet) m/z 1411.1871 ($[M + Cs]^+$, $C_{54}H_{44}F_{10}N_{10}O_{16}Cs$, calcd 1411.1831).

Compound 5. A mixture of **9** (72 mg, 0.076 mmol) and 10% Pd/C (50 mg) in anhydrous DMF (10 mL) was stirred under H_2 (10−20 psi) at room temperature for 5 h. The reaction mixture was filtered under Ar and concentrated under high vacuum at room temperature. The residue was dissolved in a mixture of anhydrous degassed CH_2Cl_2 (10 mL) and NEt_3 (0.5 mL, 4 mmol). This solution was added to a solution of 4-biphenylcarbonyl chloride (70 mg, 0.30 mmol) in anhydrous degassed CH_2Cl_2 (5 mL) at −78 °C. After 15 min, the cooling bath was removed and stirring was continued at room temperature for 20 h. The reaction mixture was diluted with $CHCl_3$ (100 mL), washed with saturated aqueous $NaHCO_3$, dried over anhydrous $MgSO_4$, and concentrated. Flash chromatography (SiO_2, $CHCl_3$/MeOH, 100:1) gave slightly impure **5** (79 mg, 0.063 mmol, 81%). To get highest purity material, the white solid was washed with EtOAc (0.4 mL), centrifuged, the supernatant decanted, and dried yielding **5** (56 mg, 0.045 mmol, 59%). Mp >300 °C (dec). TLC ($CHCl_3$/MeOH 10:1) R_f 0.59. IR (KBr, cm^{-1}) 3283w, 2984w, 1745s, 1656w, 1609w, 1487m, 1454m, 1369m, 1279s, 1256s, 1179w, 1084m, 1019m, 907m. ^{1}H NMR (400 MHz, DMSO-d_6) 9.89 (br. s, 2H), 8.01 (m, 4H), 7.75−7.60 (m, 8H), 7.42 (m, 6H), 6.73 (br. m, 4H), 5.83 (d, J = 15.8 Hz, 1H), 5.76 (d, J = 15.8 Hz, 1H), 5.33 (d, J = 15.9 Hz, 2H), 4.73 (d, J = 14.6 Hz, 2H), 4.58 (d, J = 15.8 Hz, 1H), 4.45 (d, J = 15.9 Hz, 1H), 4.25−4.00 (m, 12H), 3.75 (s, 6H), 1.25−1.10 (m, 12H) ppm. ^{13}C NMR (100 MHz, DMSO-d_6) 167.1, 165.9, 165.0, 155.6, 155.3, 154.8, 144.0, 139.9, 134.8, 133.9, 129.9, 129.3, 129.0, 128.7, 127.7, 127.4, 125.1, 111.9, 80.7, 79.4, 65.3, 64.7, 56.7, 48.4, 48.2, 36.9, 14.5, 14.4 ppm (only 28 of the 30 expected resonances were observed). MS (FAB, Magic Bullet) m/z 1252 (6, $[M + H]^+$), 181 (100). HR-MS (FAB, Magic Bullet) m/z 1384.3425 ($[M + Cs]^+$, $^{12}C_{65}{}^{13}CH_{62}N_{10}O_{16}Cs$, calcd 1384.3433).

Compound 6. A mixture of **9** (190 mg, 0.20 mmol) and 10% Pd/C (100 mg) in anhydrous DMF (20 mL) was stirred under H_2 (10−20 psi) at room temperature for 5 h. The reaction mixture was filtered under Ar and concentrated under high vacuum at room temperature. The residue was dissolved in a mixture of anhydrous degassed CH_2Cl_2 (10 mL) and NEt_3 (1.4 mL, 10 mmol). This solution was added to a solution of acetyl chloride (63 mg, 0.8 mmol) in anhydrous degassed CH_2Cl_2 (10 mL) at −78 °C. After 15 min, the cooling bath was removed and stirring was continued at room temperature for 3 h. The reaction mixture was diluted with $CHCl_3$ (200 mL), washed with saturated $NaHCO_3$, dried over anhydrous $MgSO_4$, and concentrated. Flash chromatography (SiO_2, $CHCl_3$/MeOH, 50:1) gave slightly impure **6** (193 mg, 0.198 mmol, 99%). To get highest purity material, the white solid was washed with EtOAc (0.5 mL), centrifuged, the supernatant decanted, and dried yielding **6** (165 mg, 0.170 mmol, 85%). Mp > 300 °C (dec). TLC ($CHCl_3$/MeOH 25:1) R_f 0.12. IR (KBr, cm^{-1}) 3320w, 3243w, 2984w, 1747s, 1672m, 1602w, 1521m, 1455s, 1369m, 1260s, 1178w, 1084m, 1019m, 908m. ^{1}H NMR (400 MHz, DMSO-d_6) 9.45 (s, 2H), 6.90 (br. m, 2H), 6.81 (br. m, 2H), 5.78 (d, J = 16.1 Hz, 2H), 5.19 (d, J = 15.6 Hz, 2H), 4.71 (d, J = 16.1 Hz, 2H), 4.50 (d, J = 16.1 Hz, 1H), 4.44 (d, J = 16.1 Hz, 1H), 4.25−4.05 (m, 12H), 3.74 (s, 6H), 2.03 (s, 6H), 1.22(t, J = 7.1 Hz, 6H), 1.15 (t, J = 7.1 Hz, 6H) ppm. ^{13}C NMR (100 MHz, DMSO-d_6) 169.0, 165.1, 164.1, 154.5, 154.3, 154.1, 133.3, 128.4, 126.9, 124.2, 111.4, 79.7, 78.6, 64.4, 63.8, 56.0, 47.4, 47.3, 36.2, 22.8, 13.64, 13.57 ppm (only 22 of the 23 expected resonances were observed). MS (FAB, Magic Bullet) m/z 975 (55, $[M + H]^+$), 233 (100). HR-MS (FAB, Magic Bullet) m/z 1107.2466 ($[M + Cs]^+$, $C_{44}H_{50}N_{10}O_{16}Cs$, calcd 1107.2461).

Compound 7. A mixture of **9** (72 mg, 0.076 mmol) and 10% Pd/C (50 mg) in anhydrous DMF (10 mL) was stirred under H_2 (10−20 psi) at room temperature for 5 h. The reaction mixture was filtered under Ar and concentrated under high vacuum at room temperature. The residue was dissolved in a mixture of anhydrous degassed CH_2Cl_2 (10 mL) and NEt_3 (0.5 mL, 4 mmol). This solution was added to a solution of pivaloyl chloride (37 mg, 0.30 mmol) in anhydrous degassed CH_2Cl_2 (5 mL) at −78 °C. After 15 min, the cooling bath was removed and stirring was continued at room temperature for 3 h. The reaction mixture was diluted with $CHCl_3$ (100 mL), washed with saturated $NaHCO_3$, dried over anhydrous $MgSO_4$, and concentrated. Flash chromatography (SiO_2, $CHCl_3$/MeOH, 100:1) gave slightly impure **9** (77 mg, 0.073 mmol, 96%). To get highest purity material, the white solid was washed with EtOAc (0.4 mL), centrifuged, the supernatant decanted, and dried yielding **7** (61 mg, 0.057 mmol, 76%). Mp > 300 °C (dec). TLC ($CHCl_3$/MeOH 25:1) R_f 0.24. IR (KBr, cm^{-1}) 3355w, 2965w, 1747s, 1656m, 1599w, 1485m, 1456s, 1368m, 1257s, 1181w, 1083m, 1020m, 908m. ^{1}H NMR (400 MHz, DMSO-d_6) 9.11 (s, 2H), 6.95 (d, J = 8.9 Hz, 2H), 6.89 (d, J = 8.9 Hz, 2H), 5.72 (d, J = 16.1 Hz, 2H), 5.26 (d, J = 15.9 Hz, 2H), 4.63 (d, J = 16.3 Hz, 2H), 4.52 (d, J = 16.1 Hz, 1H), 4.40 (d, J = 16.1 Hz, 1H), 4.30−4.00 (m, 12H), 3.70 (s, 6H), 1.25−1.10 (m, 12H) ppm. ^{13}C NMR (100 MHz, DMSO-d_6) 177.0, 164.9, 163.9, 154.5, 154.3, 153.8, 134.1, 128.8, 127.6, 124.6, 111.4, 80.0, 78.5, 64.4, 63.8, 56.2, 47.4, 47.1, 38.5, 36.1, 27.3, 13.6, 13.5 ppm (only 23 of the 24 expected resonances were observed). MS (FAB, Magic Bullet) m/z 1059 (40, $[M + H]^+$), 275 (100). HR-MS (FAB, Magic Bullet) m/z 1191.3384 ($[M + Cs]^+$, $C_{50}H_{62}N_{10}O_{16}Cs$, calcd 1191.3400).

Compound 8. A mixture of **13** (128 mg, 0.2 mmol) and 10% Pd/C (100 mg) in anhydrous DMF (20 mL) was stirred under H_2 (10−20 psi) at room temperature for 6 h. The reaction mixture was filtered under Ar and concentrated under high vacuum at room temperature. The residue was dissolved in a mixture of anhydrous degassed CH_2Cl_2 (60 mL) and NEt_3 (1.4 mL, 10 mmol). This solution was added to a suspension of isonicotinoyl chloride hydrochloride (142 mg, 0.8 mmol) in anhydrous degassed CH_2Cl_2 (10 mL) at −78 °C. After 15 min, the cooling bath was removed and stirring was continued at room temperature for 18 h. The reaction mixture was diluted with $CHCl_3$ (200 mL), washed with saturated aqueous $NaHCO_3$, dried over anhydrous $MgSO_4$, and concentrated. Flash chromatography (SiO_2, $CHCl_3$/MeOH, 10:1) gave **8** (127 mg, 0.16 mmol, 83%). Mp >300 °C (dec). TLC ($CHCl_3$/MeOH 10:1) R_f 0.31. IR (KBr, cm^{-1}) 3326m, 2985w, 1736s, 1702s, 1675s, 1597w, 1522s, 1471s, 1385w, 1270s, 1136w, 1077m, 1023m, 916m. ^{1}H NMR (400 MHz, DMSO-d_6) 10.11-(s, 2H), 8.65 (m, 4H), 7.78 (m, 4H), 7.22 (d, J = 8.8 Hz, 2H), 6.91 (d, J = 8.8 Hz, 2H), 5.20 (d, J = 16.1 Hz, 2H), 4.76 (d, J = 16.3 Hz, 2H), 4.25−4.10 (m, 8H), 3.75 (s, 6H), 1.25−1.10 (t, J = 7.1 Hz, 6H) ppm. ^{13}C NMR (100 MHz, DMSO-d_6) 165.6, 164.5, 157.1, 155.6, 155.1, 150.7, 141.8, 133.9, 128.3, 127.2, 126.6, 121.8, 112.1, 80.5, 64.0, 56.7, 36.8, 14.2 ppm (only 18 of the 19 expected resonances were observed). MS (FAB, Magic Bullet) m/z 791 (100, $[M + H]^+$). HR-MS (FAB, Magic Bullet) m/z 791.2808 ($[M + H]^+$, $C_{40}H_{39}N_8O_{10}$, calcd 791.2789). Anal. calcd for $C_{40}H_{39}N_8O_{10}$ (790.78), C 60.75, H 4.84. Found, C 60.66, H 4.91.

Compounds (±)-12 and 13. Compound **10** (2.10 g, 7.37 mmol) was dissolved in anhydrous DMSO (100 mL) under N_2, and *t*-BuOK (3.31 g, 29.5 mmol) was added. After the reaction was stirred for 15 min, **11** (5.00 g, 14.74 mmol) was added in one portion and stirring was continued for 3 h. The reaction mixture was poured into 0.1 N HCl (1 L) and extracted with EtOAc (3 × 400 mL). The extracts were washed with brine and dried over anhydrous $MgSO_4$. After filtration and rotary evaporation, the residue was purified by flash chromatography (SiO_2, $CHCl_3$/EtOAc 6:1) to give (±)-**12** (0.300 g, 0.468 mmol, 6.4%) and **13** (0.300 g, 0.468 mmol, 6.4%) as solids. Compound (±)-

12: Mp 296 °C. TLC ($CHCl_3$/EtOAc, 6:1) R_f 0.35. IR (KBr, cm^{-1}) 2982w, 2948w, 2909w, 1748s, 1720s, 1650m, 1635m, 1581m, 1518s, 1456s, 1429s, 1363m, 1316m, 1278s, 1149m, 1068s, 1017m. ^1H NMR (400 MHz, $CDCl_3$) 7.69 (d, $J = 9.3$ Hz, 2H), 6.77 (d, $J = 9.3$ Hz, 2H), 5.53 (d, $J = 16.8$ Hz, 2H), 5.46 (d, $J = 16.1$ Hz, 2H), 4.39 (d, $J = 16.8$ Hz, 2H), 4.10 (d, $J = 16.1$ Hz, 2H), 4.24 (q, $J = 7.1$ Hz, 4H), 3.87 (s, 6H), 1.30 (t, $J = 7.1$ Hz, 6H) ppm. ^{13}C NMR (100 MHz, DMSO-d_6) 165.3, 159.8, 155.5, 143.7, 133.6, 127.1, 126.3, 111.8, 79.9, 64.1, 57.2, 38.5, 36.1, 14.1 ppm. MS (FAB, Magic Bullet) *m*/*z* 641 (100, $[M + H]^+$). HR-MS (FAB, Magic Bullet) *m*/*z* 641.1835 ($[M + H]^+$, $C_{28}H_{29}N_6O_{12}$, calcd 641.1843). Compound **13**: Mp 314−315 °C. TLC ($CHCl_3$/EtOAc, 61) R_f 0.23. IR (KBr, cm^{-1}) 2979w, 2913w, 2850w, 1748s, 1724s, 1650w, 1631w, 1600w, 1581m, 1518s, 1460s, 1429s, 1363m, 1340m, 1316m, 1278s, 1153m, 1072m, 1021m. ^1H NMR (400 MHz, DMSO-d_6) 7.64 (d, $J = 9.2$ Hz, 2H), 6.83 (d, $J = 9.2$ Hz, 2H), 5.25 (d, $J = 16.1$ Hz, 2H), 5.11 (d, $J = 16.6$ Hz, 2H), 4.63 (d, $J = 16.6$ Hz, 2H), 4.30 (d, $J = 16.1$ Hz, 2H), 4.24 (q, $J = 7.1$ Hz, 4H), 3.74 (s, 6H), 1.24 (t, $J = 7.1$ Hz, 6H) ppm. ^{13}C NMR (100 MHz, DMSO-d_6) 165.2, 159.9, 155.6, 155.5, 143.4, 133.5, 127.2, 126.3, 111.7, 79.9, 64.1, 57.1, 38.5, 36.3, 14.1 ppm. MS (FAB, Magic Bullet) *m*/*z* 641 (100, $[M + H]^+$). HR-MS (FAB, Magic Bullet) *m*/*z* 641.1827 ($[M + H]^+$, $C_{28}H_{29}N_6O_{12}$, calcd 641.1843).

NMR Experiments. For the ^1H NMR experiments, the temperature was maintained (± 0.5 K) with a Bruker eurotherm module that had been calibrated using the separation of the resonances of methanol. For self-association measurements, a series of spectra were recorded at a series of concentrations (10−0.05 mM). The tabulated values of chemical shift versus concentration were fitted using a self-association model implemented within Scientist (MicroMath Scientific Software, Salt Lake City, UT). Selective 1D ROESY spectra were acquired using the pulse sequences supplied by Bruker. The heterodimer exchange equilibrium constant measurements were performed at 1 mM concentration of each component. Spectra were referenced relative to residual solvent resonances or external tetramethylsilane.

Gel Permeation Chromatography. GPC experiments were performed on a Beckman System Gold HPLC with a Shodex OHpak SB-802.5HQ (8 mm × 30 cm) GPC column (Phenomenex, Torrance, CA) using UV/Vis detection at 254 nm. The GPC column was calibrated by triplicate measurements of the migration time of commercially available polystyrene standards (Polymer Laboratories, MW = 162, 580, 925, 1260, 2350, and 4920). The measurements were performed using 20 μL injections of 2 mM solutions in $CHCl_3$.

X-ray Crystal Structures for 1 and 2. The crystal structure of **1** has been reported previously[25] and deposited with the Cambridge Crystallographic Data Centre (CCDC-187956). Detailed descriptions of the data collection, solution, and refinement of the structure of **2** can be found in the Supporting Information. Crystal data for **2**: $[C_{52}H_{52}N_{12}O_{16}][CH_3OH]_{0.15}[H_2O]_{0.85}$ (1121.18); Monoclinic, space group P2(1)/c; colorless block, $a = 20.2117(7)$ Å, $b = 15.3609(5)$ Å, $c = 17.3442(6)$ Å; $V = 5010.1(3)$ $Å^3$; $Z = 4$; $T = 173(2)$ K; $R(F) = 0.0948$; GOF on $F^2 = 1.096$.

Acknowledgment. This work was supported by the National Institutes of Health (GM61854) and the University of Maryland. L.I. is a Cottrell Scholar of Research Corporation. We thank the reviewers for their insightful comments.

Supporting Information Available: Crystallographic data for **2**, MMFF-minimized structure of **8·8**, NMR data for **2·2** as a function of solvent, the models used by Scientist, and selected ^1H and ^{13}C NMR spectra (PDF, CIF). This material is available free of charge via the Internet at http://pubs.acs.org.

JA0486972